



Sinomenine Hydrochloride Protects IgA Nephropathy Through Regulating Cell Growth and Apoptosis of T and B Lymphocytes

Jun-Jian Li ^{1,2,*}, Li Li^{2,*}, Shuang Li^{2,3}, Xin-Yi Tang², Hui-Feng Sun¹, Jian-Xin Liu ²

¹School of Pharmacy, Heilongjiang University of Chinese Medicine, Harbin, Heilongjiang, People's Republic of China; ²School of Pharmaceutical Sciences, School of Basic Medical Sciences, Hunan Provincial Key Laboratory of Dong Medicine, Hunan University of Medicine, Huaihua, People's Republic of China; ³Harbin Voolga Technology Co., Ltd., Harbin, People's Republic of China

*These authors contributed equally to this work

Correspondence: Hui-Feng Sun, School of Pharmacy, Heilongjiang University of Chinese Medicine, Harbin, Heilongjiang, 150040, People's Republic of China, Email 13936243669@139.com; Jian-Xin Liu, School of Pharmaceutical Sciences, School of Basic Medical Sciences, Hunan Provincial Key Laboratory of Dong Medicine, Hunan University of Medicine, Huaihua, 41800, People's Republic of China, Fax +745-2381210, Email liujianxin3385@126.com

Purpose: Sinomenine hydrochloride (SH) is used to treat chronic inflammatory diseases such as rheumatoid arthritis and may also be efficacious against Immunoglobulin A nephropathy (IgAN). However, no trial has investigated the molecular mechanism of SH on IgAN. Therefore, this study aims to investigate the effect and mechanism of SH on IgAN.

Methods: The pathological changes and IgA and C3 depositions in the kidney of an IgAN rat model were detected by periodic acid-Schiff (PAS) and direct immunofluorescence staining. After extracting T and B cells using immunomagnetic beads, we assessed their purity, cell cycle phase, and apoptosis stage through flow cytometry. Furthermore, we quantified cell cycle-related and apoptosis-associated proteins by Western blotting.

Results: SH reduced IgA and C3 depositions in stage 4 IgAN, thereby decreasing inflammatory cellular infiltration and mesangial injury in an IgAN model induced using heteroproteins. Furthermore, SH arrested the cell cycle of lymphocytes T and B from the spleen of IgAN rats. Regarding the mechanism, our results demonstrated that SH regulated the Cyclin D1 and Cyclin E1 protein levels for arresting the cell cycle and it also regulated Bax and Bcl-2 protein levels, thus increasing Cleaved caspase-3 protein levels in Jurkat T and Ramos B cells.

Conclusion: SH exerts a dual regulation on the cell cycle and apoptosis of T and B cells by controlling cell cycle-related and apoptosis-associated proteins; it also reduces inflammatory cellular infiltration and mesangial proliferation. These are the major mechanisms of SH in IgAN.

Keywords: sinomenine hydrochloride, cell cycle, apoptosis, IgAN, Jurkat T and Ramos B cells

Introduction

IgA nephropathy (IgAN) is a primary glomerulonephritis¹ characterized by hematuria and^{2,3} nephrotic syndrome, in particular proteinuria.⁴ It is often treated by kidney transplantation⁵ after the renal disease reaches its end state. However, the risk of IgAN recurrence remains after transplantation.⁶ Interestingly, IgAN deposition disappeared when the kidneys of IgAN patients were transplanted into patients without IgAN,^{7,8} implying that the main location of the pathology was the immune system rather than the kidney.⁹

As immunoglobulin A (IgA) is mainly produced by plasmacytes,¹⁰ IgAN has been associated with the immune system since it was discovered.¹¹ However, before 2022, IgAN treatment strategies focused on alleviating kidney and mesangial tissue injuries rather than targeting the immune system to reduce IgA production.¹² In fact, decreasing kidney damage has demonstrated efficacy in treating IgAN, but it also has some drawbacks. Thus, decreasing inflammatory

cellular infiltration and IgA and C3 deposition in the kidney is effective, but IgAN treatments based on new strategies need to be developed.

Spleen B cells in the intestine are mostly IgA⁺ plasma cells.¹³ In the initial stage of IgAN, the mucosal infection destroying the defense functions of the mucosal barrier leads to antigen presentation to B lymphocytes,¹⁴ which then differentiate into plasma cells and secrete IgA through T cell dependent and independent modes.¹⁵ Besides, the abnormal regulation of bone marrow and dysregulation of B cell and plasmocyte homing receptor increase IgA1 abnormal glycosylation.¹⁶ B cell proliferation is known to be associated with the risk and prognosis of IgAN.¹⁷ The number of CD19⁺ B cells increased in IgAN patients compared to healthy controls.¹⁸ As dysregulation of B cell promotes IgAN progression by increasing IgA1 abnormal glycosylation and IgA production, a new strategy, B cell depletion, has been considered for treating IgAN and applied in a clinical setting.¹⁹ In addition, monomer compounds from traditional Chinese medicine such as tripterygium glycosides have been shown to have the potential to treat IgAN by reducing the proliferation of B cells.²⁰ Nano-preparations such as orange-derived and dexamethasone-encapsulated extracellular vesicles reduced proteinuria and alleviated pathological lesions in IgA nephropathy by targeting B lymphocytes.²¹

T cells are also very important and extensively involved in IgAN progression.²² The dysregulation of T cell can promote IgA1 abnormal glycosylation and IgA production and ultimately leads to increased levels of the immune complex Gd-IgA1. In addition, T cell infiltration is involved in the renal injury process. As T cells promotes IgA progression, the number of CD4 primary T cells and regulatory T cells increased;²³ Th cells are more activated in IgAN patients.²⁴ Hence, targeting the T cell is desirable.²⁵ Decoy receptor 3 (DCR3), a potential immune regulator, prevents the progression of IgAN in B cell-deficient mice by inhibiting systemic T cell activation and proliferation.²⁶ Acteoside can alleviate mesangial cell inflammatory injury by modulating Th2 lymphocytes chemotaxis and proliferation.²⁷ Therefore, drugs depleting B and T cells hold potential for treating IgAN.

The cell cycle is the mechanism of cell proliferation and is regulated by Cyclin proteins, including Cyclin E1 and Cyclin D1.²⁸ Moreover, a dysregulation of Cyclins can arrest the cell cycle.

Apoptosis, an autonomously programmed cell death, is a gene-controlled process maintaining the stability of the internal environment; it was first reported in 1972.²⁹ It is regulated by various proteins, such as Bax (BCL2-Associated X), Bcl-2 (B-cell lymphoma-2), and Cleaved caspase-3.³⁰

Sinomenine is a morphinan alkaloid extracted from the traditional Chinese medicine *Sinomenium acutum* (Thunb.), and its medicinal hydrochloride is sinomenine hydrochloride (SH). SH is the main component of Zhengqing Fengtongning sustained-release tablets, which is the principal Chinese herbal medicine for treating rheumatoid arthritis by regulating the secretion of inflammatory cytokines and monocyte/macrophage subsets, and has shown therapeutic effect on kidney diseases.³¹ Previous studies have showed that SH significantly inhibits the production of pro-inflammatory cytokines, prostaglandin E2 and NO through down-regulating the expression of membrane-associated PGE2 synthase, suppresses macrophage migration by down-regulating Src/FAK/P130Cas activation, and inhibits the proliferation and activity of macrophages and lymphocytes.^{32,33} However, the mechanism of SH in IgAN remains unknown. This study is the first to document the effect and molecular mechanism of SH on IgAN.

Material and Methods

Reagents

Sinomenine hydrochloride (purity >98%) was offered by Huaihua Zhenghao Pharmaceutical Co., Ltd. Lipopolysaccharide (LPS, L2880), Losartan (Y0001076), Triton-X-100 (X100), Bovine serum albumin (BSA, A9647) were all obtained from Sigma, USA. Ramos [RA 1] (CL-0483) cells were kindly provided by Procell LifeScience&Technology Co., Ltd. Jurkat T (Clone E6-1) cells were obtained from National Collection of Authenticated Cell Cultures. CellTiter 96[®] Aqueous One Solution Cell Proliferation Assay (MTS, G3580) was purchased from Promega (Madison, WI, USA). ECL Western Blotting Substrate (211,020–65) was purchased from Advansta, RIPA Lysis Buffer (B10C00130) was obtained from Beijing Dingguo Changsheng Biotechnology Co., Ltd. SDS-PAGE Sample Loading Buffer 5x (BL502A) was purchased from Biosharp Life Science. Mouse anti- β -actin polyclonal antibody (10,021,787), Rat FITC labeled IgA primary antibody (ab97234), and FITC labeled C3 primary antibody (ab4212) were purchased from Abcam. CyclinD1 (D0918) and Bcl-2 (H0318) Mouse antibody

were all obtained from Santa Cruz Biotechnology. CyclinE1 (2080S), Caspase-3 (9662S), and Bax (2772S) Rabbit antibody were all obtained from Cell Signaling Technology. Frozen section OCT embedding agent (4583) was obtained from Sakura, USA. Goat serum (CW0130S) was purchased from Beijing Kangwei Century Biotechnology Co., Ltd. MidiMACS™ Starting Kits (LS: 130–042–301, LD: 130–090–329), Pan T Cell MicroBeads (130–090–320), and CD45RA MicroBeads (130–090–494) were all obtained from Miltenyi Biotec Inc. CD3 Monoclonal Antibody (17–0030–82) and CD45R (B220) Monoclonal Antibody (12–0460–82) were all obtained from Thermo Fisher Scientific.

Animals and Ethics

Male SD rats (SPF grade, 150 ±10g, License key: SCXK 2019–0004) were purchased from Hunan Slake Jingda Experimental Animal Co., Ltd. All animal experiments were approved by the Ethics Committee of the National Research Centre and the Ethics Committee of Hunan University of Medicine [2022(A01018)]. For the well-being of the rats, the feeding, nursing and testing of all animals were strictly handled in accordance with the National Institutes of Health Guide for the Care and Use of Laboratory Animals. They were afforded unrestricted access to both food and water and received nursing by the veterinary. All personnel involved in the care and use of animals were fully educated and trained in the basic principles of laboratory animal science to ensure that surgical treatment was sterile and warm. Isoflurane inhalation anesthesia was used to relieve pain in animals.

Animals Sample Size Calculation

The number of animals per group was calculated using the resource equation approach as described by Georgios D Panos and Frank M Boeckler,³⁴ the limit of error degrees of freedom (X) between 10 and 20 was open to interpretation. Based on this calculation, a minimum of 5 and maximum of 6 animals were required for this study. Due to the time and difficulty of model building, we performed the experiment ($n = 7$, $X = 24$), which would be of an appropriate size, albeit just over the recommended upper limit.³⁵

IgAN Rat Model

After one week of adaptive feeding, male SD rats received bovine serum albumin (BSA, 600 mg/kg) for 8 weeks. During the first week, they received Freund's complete adjuvant containing 0.2 mg BSA (0.2 mL per rat) by subcutaneous injection. The same solution was then administered through intraperitoneal injections. Meanwhile, each rat received subcutaneous injections of 0.1 mL CCl₄ and 0.5 mL Castor oil once a week for 8 weeks, and lipopolysaccharide (0.025 mg) was administered through tail vein injections in the sixth and eighth weeks to establish the IgAN model. The successfully modeled rats were divided into the IgAN group, high SH dose group (SH-H, 100 mg/kg/d), low SH dose group (SH-L, 25 mg/kg/d), and Losartan group (5 mg/kg/d). SH and Losartan were dissolved in purified water to achieve the appropriate dose. Normal group and IgAN group were administrated with equal volume of purified water. Treatments were administered once a day for 6 weeks. The partial renal cortices placed in standard fixing solution were embedded in paraffin.

Periodic Acid–Schiff (PAS) Staining

After graded alcohol dehydration, the paraffin sections of rat kidney tissue (6 μm) were stained using a PAS staining kit. Images were obtained using a light microscope and characterized according to Lee's classification of IgA nephropathy.

Direct Immunofluorescence Staining

Renal cortices were longitudinally cut into 6 μm-thick slices. After acetone fixation (15 min), tissue permeabilization (0.5% Triton-X-100), fixing (phosphate-buffered saline (PBS) with 5% goat serum, room temperature, 30 min), FITC-labeled rat IgA and C3 primary antibody (1:100, 50–100 μL) were added for incubation overnight at 4 °C. Then, Fluorescent Mounting Media was added dropwise, and neutral gum sealing was performed. Images were recorded under a fluorescence upright microscope, and IgA and C3 deposition was analyzed using Image-Pro Plus 6.0.

Magnetic-Activated Cell Sorting

Experimental cells (1×10^7) were centrifuged for 10 min. After discarding the supernatant, samples were incubated with 20 μ L Pan T Cell MicroBeads/20 μ L CD45RA MicroBeads for 15 min at 2–8 °C. After centrifuging and discarding the supernatant, samples were resuspended by 500 μ L buffer. After moisturizing and washing the pipes, the magnetically labeled single-cell suspension was loaded into the separation column. After washing with 5 mL buffer, the cells were eluted to obtain the T and B lymphocytes separately.

Cell Culture

Ramos B and Jurkat T cells were subjected to incubate in complete medium consisting of RPMI 1640, 10% fetal bovine serum (FBS) and 1% penicillin-streptomycin in an incubator comprising 5% CO₂ at a temperature of 37 °C. SH was dissolved in RPMI 1640, filtrated through a 0.22 μ m pore size membrane, and further diluted with RPMI 1640 to the tested concentrations.

Treatment of SH

After 24 h incubation with RPMI 1640 containing 1% FBS, the experimental cells (1.4×10^5 cells/mL or 2.5×10^5 cells/mL) were seeded into 96-well/6-well plates and treated with SH for 48 h. These cells were divided into groups according to the concentrations of SH.

MTS Assay

Experimental cells in good condition were incubated for 24 h, then treated with SH for 48 h in 96-well plates. After adding 10 μ L of MTS solution into each well, cells were incubated away from light in an incubator. Microplate reader was used to detect the optical density after 4 h.

Analysis of Cell Cycle

The cells incubated with SH were collected into 5 mL tubes. The experimental cells were resuspended in 1 mL of PBS and uniformly mixed. Absolute ethyl alcohol was slowly added to the experimental cells, which were then fixed by incubation in 4 °C overnight. Next, the cells were treated with a solution containing 500 μ L of precooled PBS and 20 μ L of RNase A. Finally, the cells were collected and treated with 400 μ L PI (Sigma-Aldrich Corp) and monitored by flow cytometer.

Analysis of Apoptosis

The cells treated with SH were collected into 5 mL tubes, then resuspended in Binding Buffer. Next, 100 μ L suspension of cells was transferred into a new tube. Next, these cells were treated with 5 μ L of Annexin V-FITC and 5–10 μ L of PI under dark conditions. The cells were mixed with 400 μ L of Binding Buffer and analyzed by flow cytometry.

Western Blot Assay

The proteins of cells were extracted with RIPA buffer and quantified using a BCA protein assay kit (Beyotime Biotechnology, Jiangsu, China). After separating the total protein by 15% SDS-PAGE, polyvinylidene difluoride membrane was used for protein transferring. Then, the membranes were incubated with the primary antibodies against Cyclin D1 (1:500), Cyclin E1 (1:1000), Caspase-3 (1:1000), Bax (1:1000), and Bcl-2 (1:1000) at 4 °C overnight. Then, the membrane was incubated with the secondary antibodies for 2 h. A visualizer was applied for protein quantification.

Statistical Analysis

Experimental data ($n = 7$) were statistically compared using Normality and Lognormality Tests (QQ plots) to assess data distribution and then perform Welch *t*-test, Welch-ANOVA with Games-Howell's multiple comparisons test by GraphPad Prism 9.0 ($P < 0.05$ regard as difference). Experimental data ($n = 3$ or 4) were statistically compared using bootstrapping tests by SPSS v26.0 and made by GraphPad Prism 9.0 ($P < 0.05$ regard as difference).

Table 1 Pathology Grading Results

Groups	N	Pathological grades					
		0	I	II	III	IV	V
Normal	7	7					
IgAN	7				1	5	1
SH-L	7			2	5		
SH-H	7		5	1	1		
Losartan	7		4	3			

Results

SH Notably Reduced the Pathological Manifestations in Renal Tissue of IgAN Rats

The pathological manifestations of IgAN are usually characterized by quantifying mesangial cell proliferation and inflammatory cell infiltration.³⁶ Therefore, we assessed the pathological manifestations in the renal tissue of IgAN rats by performing PAS staining. Our results confirmed that pathological manifestations, including significant mesangial cell proliferation, obvious abnormality of renal tubules, and inflammatory cell infiltration, were not present in normal rats (Table 1 and Figure 1) but were found in IgAN rats (one class III case, five class IV cases, and one class V case). Note-worthily, these pathological manifestations did lightly improve in the SH-L group and notably improve in the SH-H group (five class I cases, one class II case, and one class III case) compared with IgAN group. Finally, the mesangial cell proliferation was also improved in the Losartan group (four class I cases and three class II cases).

SH Markedly Decreased IgA and C3 Deposition in IgAN Rat Model

As IgA and C3 deposition are important feature of IgA nephropathy, we assessed the IgA and C3 deposition in IgAN rats by Direct immunofluorescence staining. The results revealed no IgA and C3 deposition in the mesangial region of normal rats. However, green IgA and C3 fluorescence appeared in the IgAN, SH-L, SH-H, and Losartan groups. The fluorescence intensity analysis showed that all the model groups had significantly more IgA and C3 deposition than the normal group. Moreover, the SH-H and Losartan had markedly less IgA and C3 deposition in rat glomeruli than the IgAN group (Table 1, Figure 2A and B).

SH Notably Arrested the Cell Cycle of T and B Cells in the Spleen

For exploring the effect of SH on T and B cells in vivo, Spleen T and B cells were extracted using Pan T Cell and CD45RA MicroBeads, and detected by flow cytometer. The purity values of T and B cells were 91.1% and 82.3%, respectively (Figure 3A). In addition, spleen T and B cells of the IgAN group had a significantly shorter G0/G1 phase

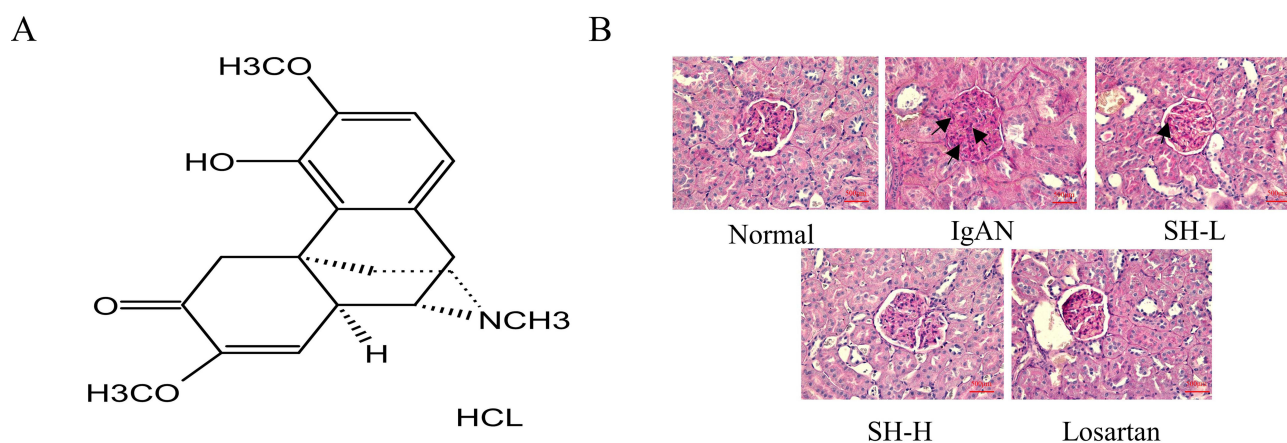


Figure 1 SH notably reduced the pathological manifestations in renal tissue of IgAN rats. (A) Chemical structure of SH. (B) Representative photographs of PAS staining of the kidney tissue ($\times 400$) of rats revealed differences between the treatment groups and the IgAN model group.

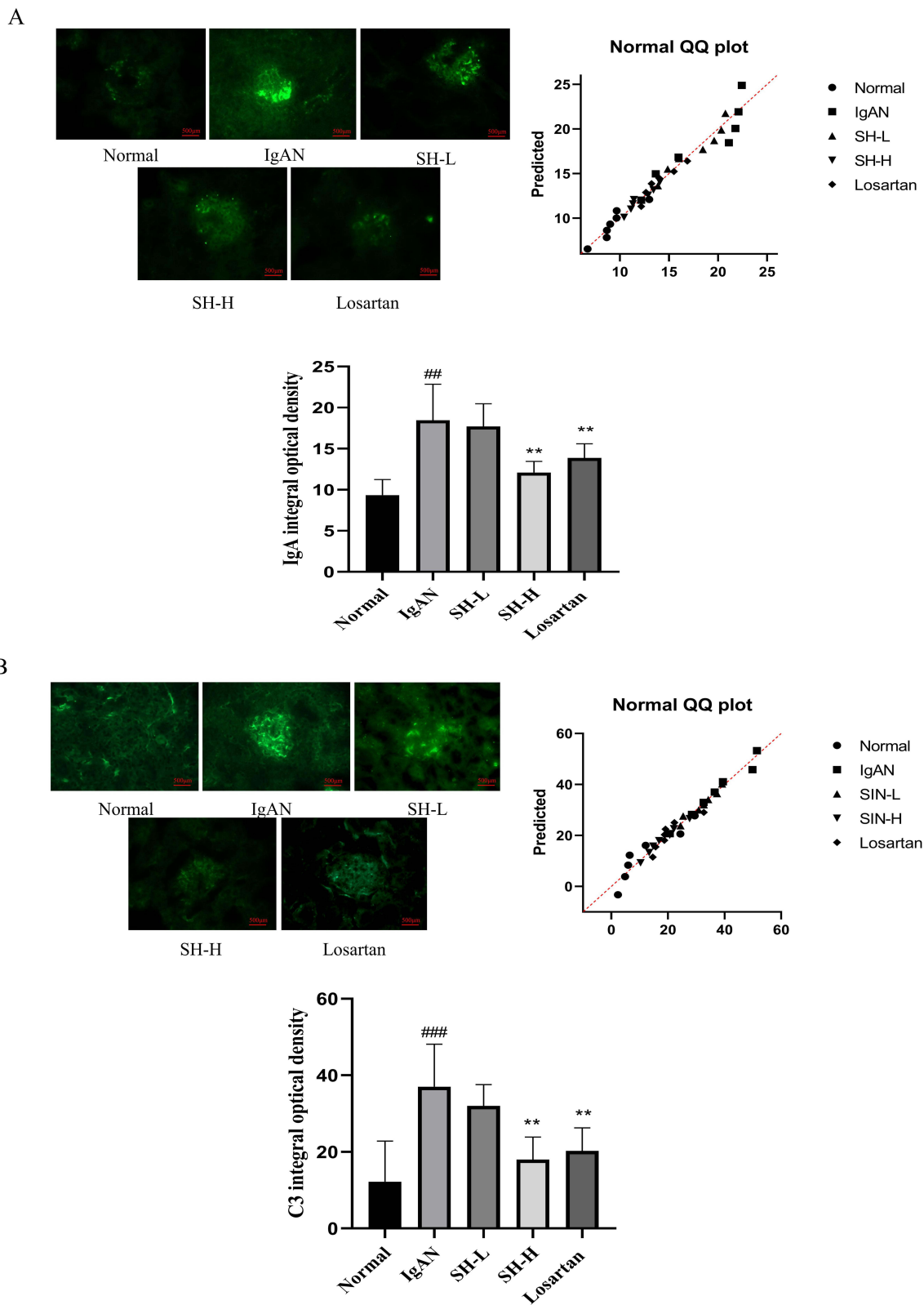


Figure 2 SH markedly decreased IgA and C3 deposition in IgAN rat model. IgA (**A**) and C3 (**B**) deposition in the IgAN model rats (n = 7) treated with SH or Losartan compared with untreated IgAN rats. The values represent the mean ± SEM (n = 7). ^{##}p < 0.01, ^{###}p < 0.001, vs normal group. ^{**}p < 0.01, vs IgAN group.

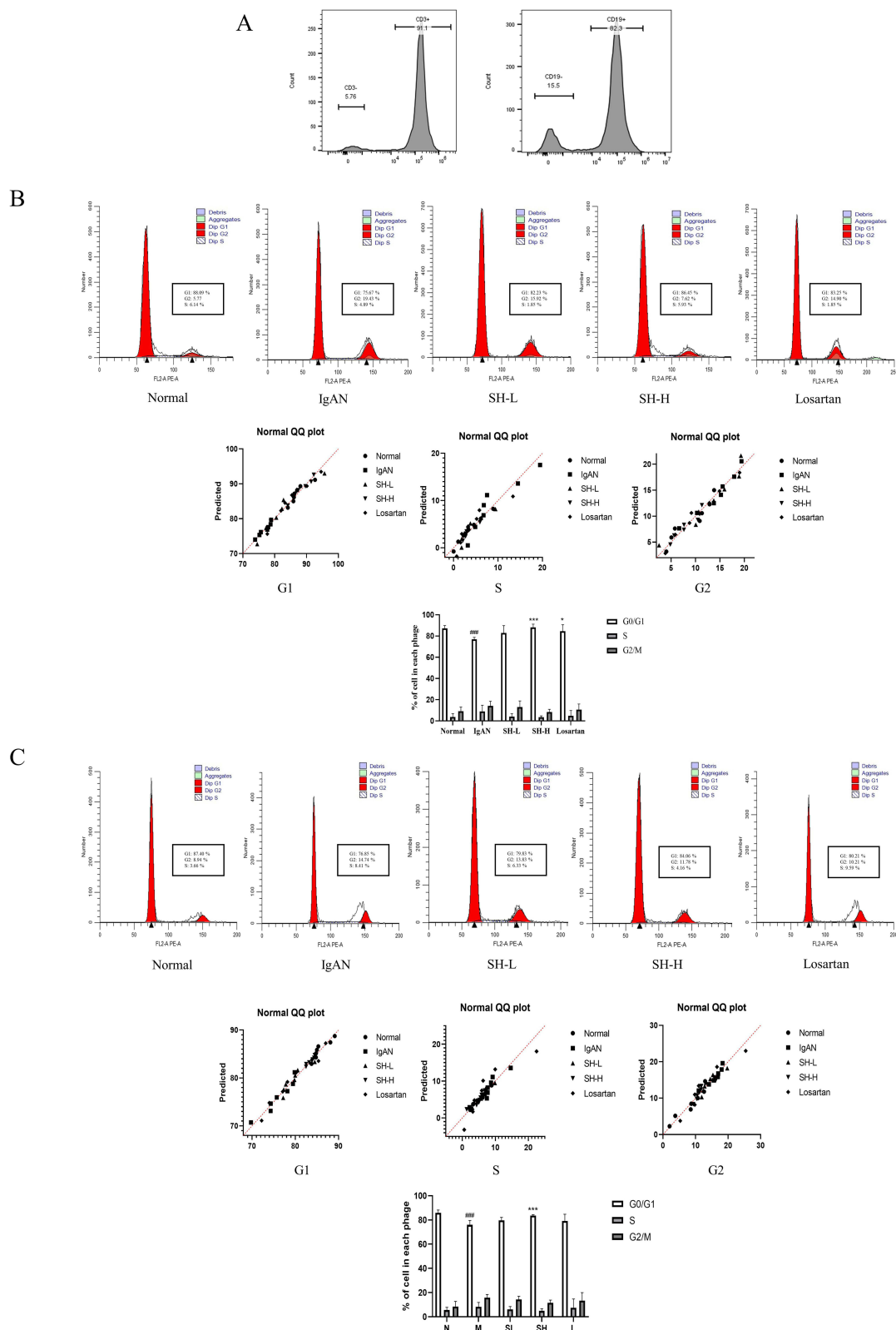


Figure 3 SH notably arrested the cell cycle of T and B cells in the spleen. The purity (**A**) and cell cycle of T (**B**) and B (**C**) cells were assessed by flow cytometry. The difference in the proportion of spleen T and B cells in each cell cycle phase treated with SH or Losartan is displayed as the mean \pm SEM ($n = 7$). $####p < 0.001$, vs normal group, $*p < 0.05$, $***p < 0.01$ vs IgAN model group.

than those of the normal group, but SH reverted this trend by arresting the G0/G1 phase. Interestingly, losartan had a weaker effect on spleen T cells than SH-H, but no significant difference on spleen B cells; SH-H was more potent on spleen T and B cells (Figure 3B and C).

SH Notably Reduced the Cell Proliferation Rate and Arrested Cell Cycle in Jurkat T and Ramos B Cells

To explore the effects of SH on T and B cells in vitro, MTS was applied to detect cell proliferation. The results indicated that SH (0.5 μ M) and SH (1 μ M) markedly reduced the proliferation of Ramos B and Jurkat T cells (Figure 4A and B). Moreover, it did not affect HUVEC cells (Figure 4C). Furthermore, these experimental cells were stained with PI and analyzed by flow cytometry. Our results showed that SH arrested the cell cycle in Jurkat T and Ramos B cells, consistent with the effect of SH on spleen T and B cells (Figure 4D and E).

SH Significantly Reduced the Cell Cycle-Related Protein Expression in Jurkat T and Ramos B Cells

The cell cycle is closely associated with proliferation and regulated by Cyclin E1 and Cyclin D1, which promote the transition from the G0/G1 phase to the S phase.³⁷ Therefore, the Western blotting was used to quantify Cyclin E1 and Cyclin D1 in Jurkat T and Ramos B cells. Our results clearly showed that SH down-regulated Cyclin E1 and Cyclin D1 protein expression (Figure 5A and B).

SH Induced Apoptosis in Jurkat T and Ramos B Cells

In order to further explore the effect of SH on T and B cell, the cells were treated by SH and incubated with Annexin V-FITC and PI. Apoptotic cells appeared in brown and green in scatter diagram. Compared with normal cells, SH (0.5 μ M) and SH (1 μ M) had markedly higher apoptosis levels in Jurkat T and Ramos B cells (Figure 6A and B).

SH Strongly Regulated the Apoptosis-Related Protein Expression in Jurkat T and Ramos B Cells

Apoptosis is a complicated process regulated by many proteins. Here, we evaluated the effects of SH on the Caspase-3, Cleaved caspase-3, Bax, and Bcl-2 protein expression by Western blot. SH markedly reduced Bcl-2 and Caspase-3 protein expression and significantly promoted Bax and Cleaved caspase-3 protein expression in Jurkat T and Ramos B cells (Figure 7A and B).

Discussion

IgAN is characterized by the deposition of the IgA (mainly IgA1) immune complex in the mesangial area.³⁸ There are three frequently used IgAN rat models: the spontaneous variant, secondary lesion, and immune inducible models. Through comparative research, we previously found that the IgAN animal model induced by heterologous proteins is relatively similar to human IgAN in terms of clinical detection indicators and pathological changes.³⁹ The IgAN animal model was established by BSA (induce IgA production in vivo), LPS (damage the liver endothelial reticular system and reduce IgA clearance), and CCl₄ (induce cirrhosis and further reduce the clearance of IgA). In this study, the IgAN animal model induced by heterologous proteins was improved by increasing injection of Freund's complete adjuvant and Freund's incomplete adjuvant containing BSA to enhance immune response induction. Our results clearly showed that IgAN model rats displayed markedly more mesangial cell proliferation and inflammatory cell infiltration than normal rats. Furthermore, IgAN model rats had significant IgA and C3 deposition in the glomerular area. These results were consistent with the IgAN pathological characteristics, indicating that the establishment of model was successful.

The pathological development of IgAN goes through four main stages: (1) B lymphocytes generate plenty of IgA1, which is little glycosylated and not easily cleared; (2) the IgA1 immune complex formed reaches the kidneys through the blood cycle; (3) the IgA1 immune complex accumulates in the mesangial area, and binds to and activates mesangial cells; (4) active mesangial cells release multiple cytokines, prompting mesangial cell proliferation and inflammatory cell infiltration, ultimately leading to kidney damage.^{40–42} Our results clearly show that SH treatment markedly reduces

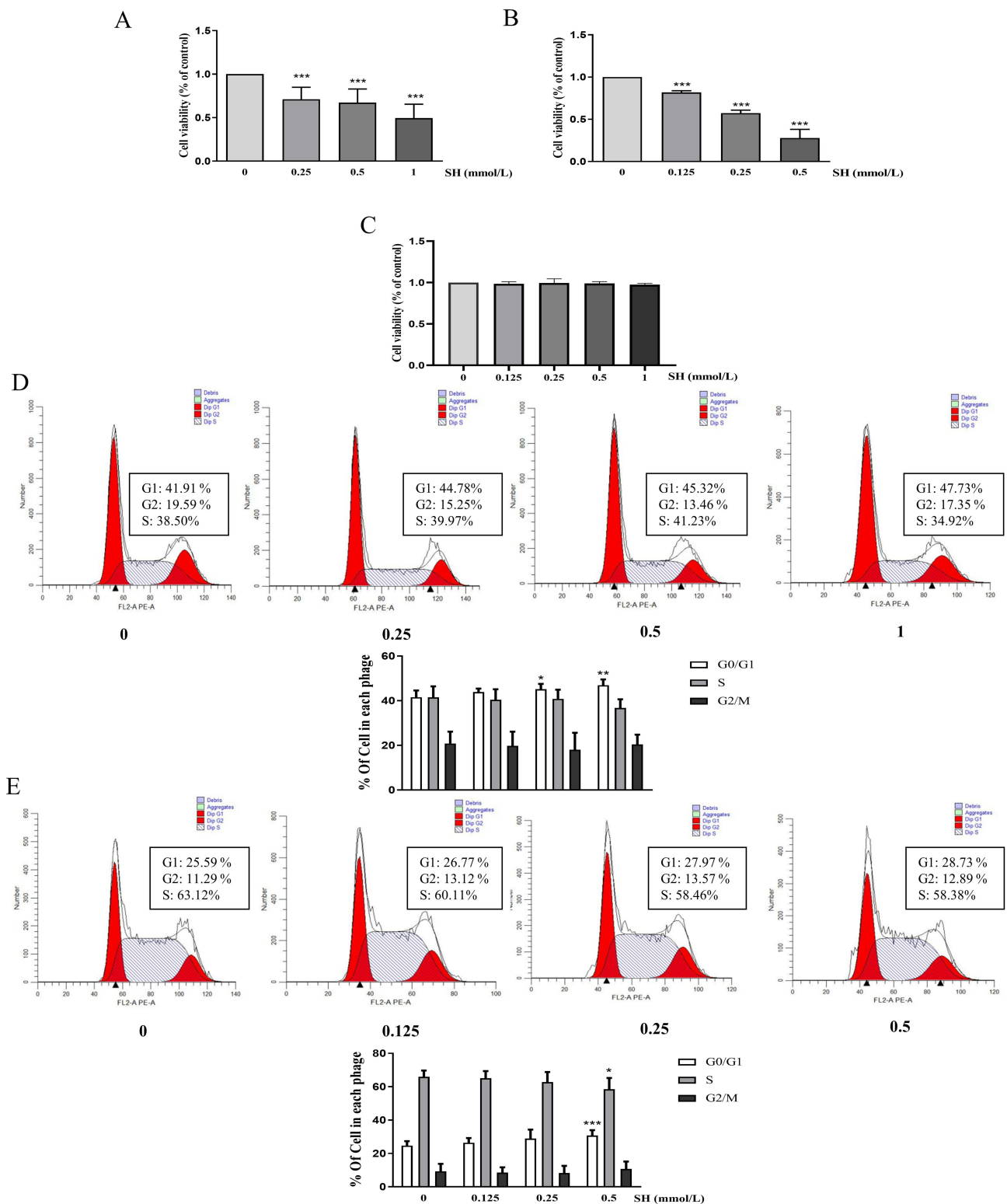
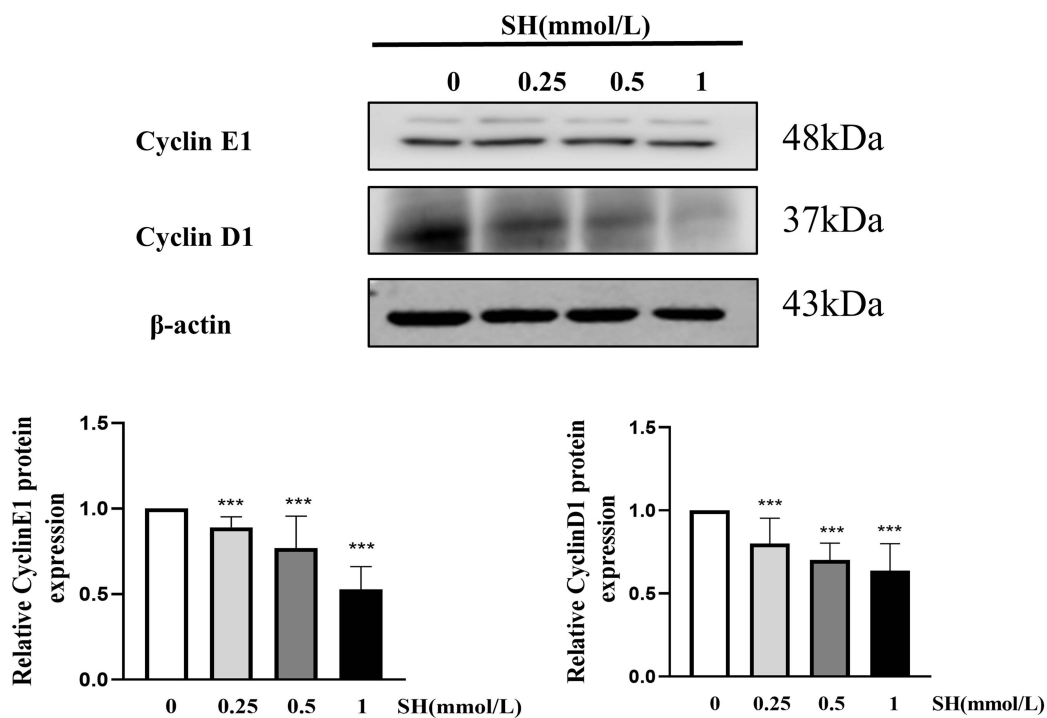


Figure 4 SH notably reduced the cell proliferation rate and arrested cell cycle in vitro. **(A)** Jurak T cells, **(B)** Ramos B cells, and **(C)** HUVEC cells are shown as the means \pm SEM (n=3). The histogram displays the flow cytometry data. The change in the proportion of **(D)** Jurkat T and **(E)** Ramos B cells in the G0/G1, S, and G2/M phases are shown as the means \pm SEM (n = 4). *p < 0.05, **p < 0.01, ***p < 0.001 vs control group.

pathological damage (mesangial cell proliferation, inflammatory cell infiltration, and IgA and C3 deposition) in rat kidney tissue. These results strongly indicated that SH has a therapeutic effect on IgAN by effectively preventing the progression of IgAN to stage 4.

A



B

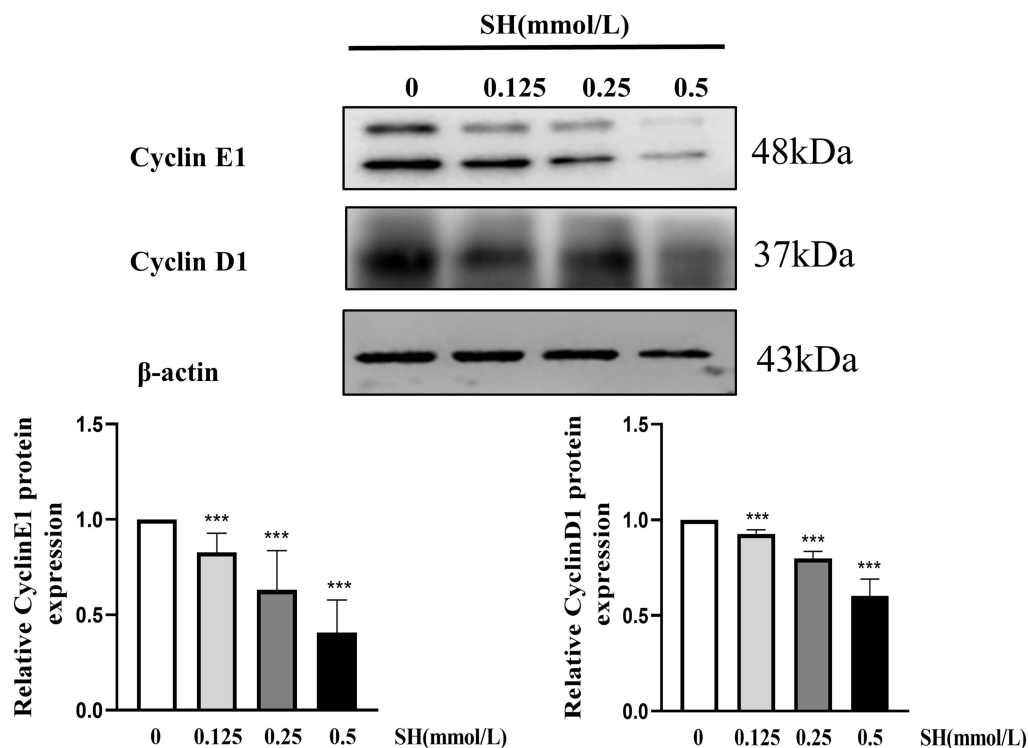
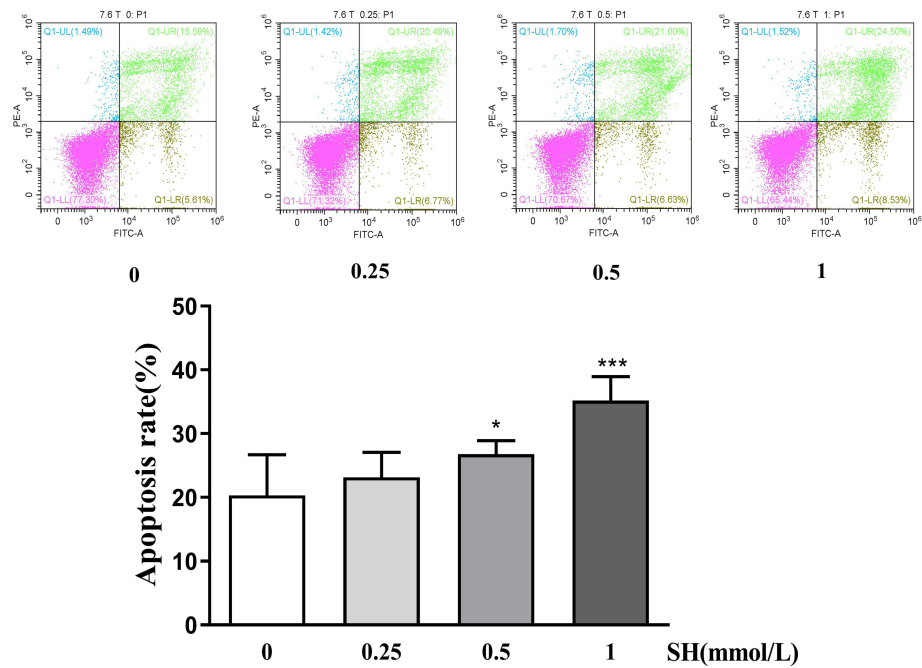


Figure 5 SH significantly reduced the cell cycle-related protein expression. Cyclin E1 and Cyclin D1 in (A) Jurkat T and (B) Ramos B cells were quantified by Western blot. The values represent the mean \pm SEM (n = 3). ***p < 0.001 vs control group.

A



B

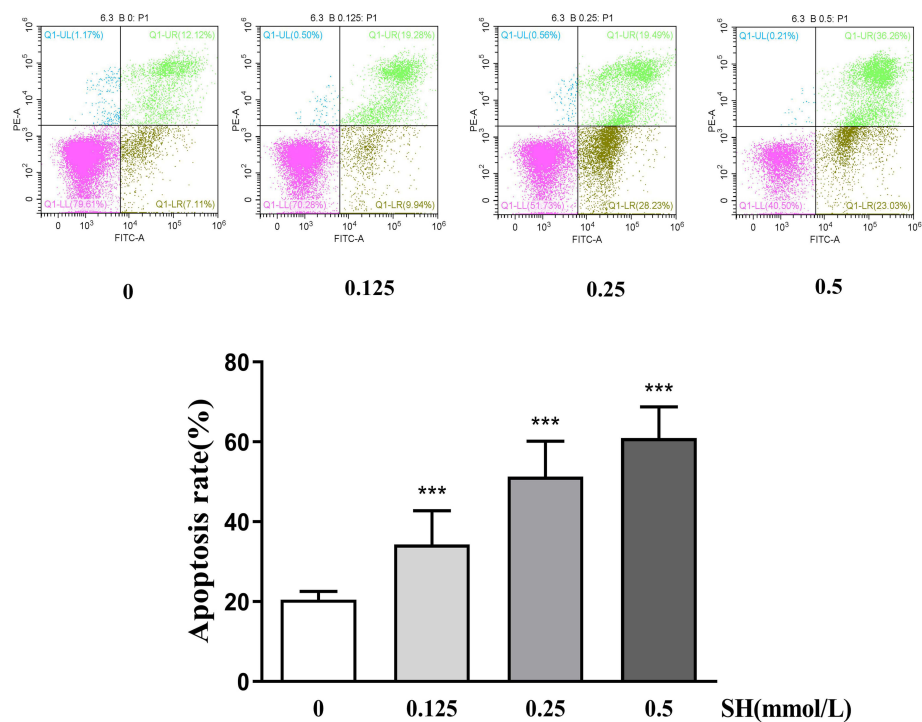


Figure 6 SH induced apoptosis in Jurkat T and Ramos B cells. The (A) Jurkat T and (B) Ramos B cells were treated with SH at different concentrations and stained with PI and Annexin V-FITC. The results are shown as the means \pm SEM (n = 4). *p < 0.05, ***p < 0.001 vs control group.

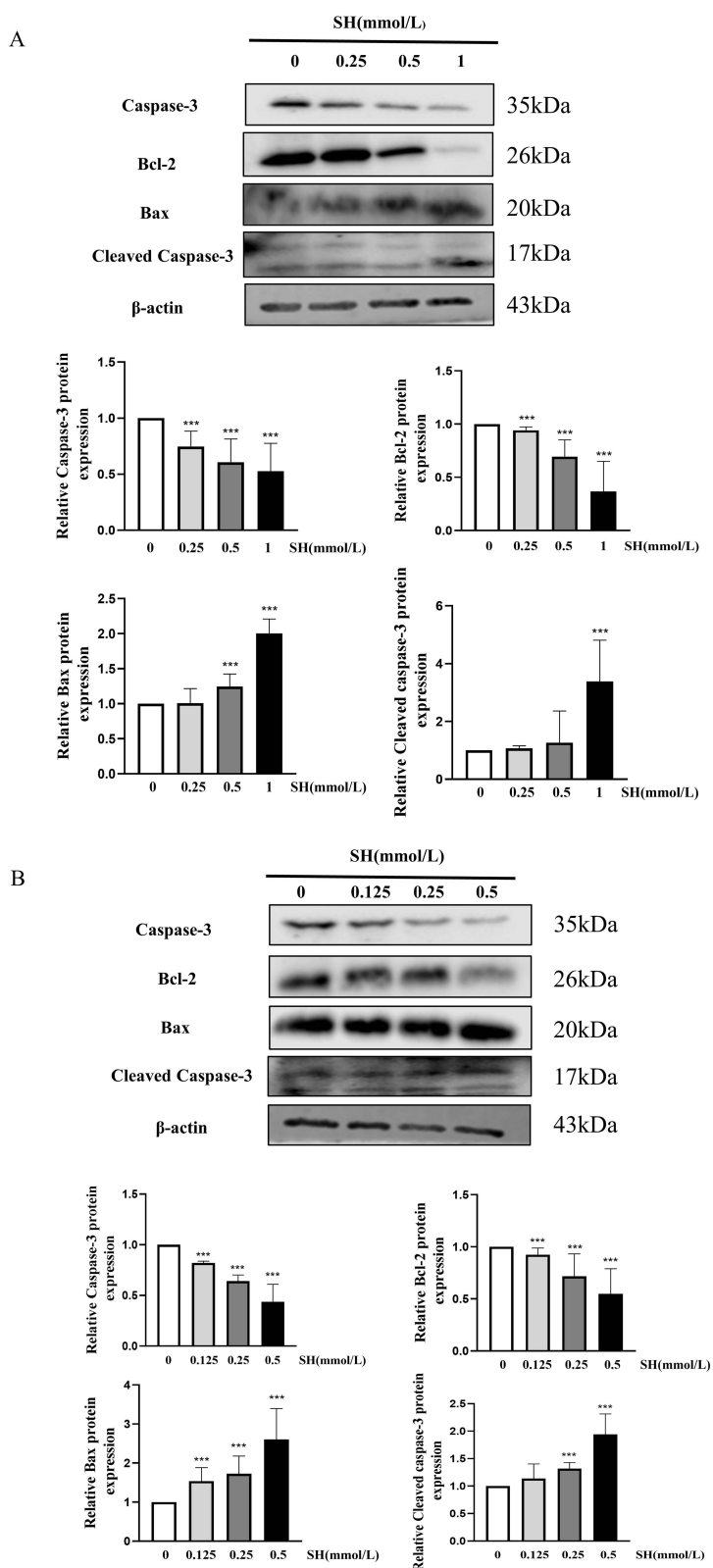


Figure 7 SH strongly regulated the apoptosis-related protein expression. Caspase 3, Cleaved caspase-3, Bax and Bcl-2 in **(A)** Jurkat T and **(B)** Ramos B cells were quantified by Western blot. The values represent the mean \pm SEM (n = 3). ***p < 0.001 vs control group.

The therapeutic strategy of IgAN mainly concentrates on the final stage of IgAN progression, usually using glucocorticoid or immunosuppressive drugs to reduce glomerular injury, along with renin–angiotensin system inhibitors,⁴³ angiotensin-converting enzyme inhibitors, and angiotensin receptor blockers to reduce the production of proteinuria.⁴⁴ However, the high proportion of IgAN patients developing end-stage renal failure highlights the deficiencies of this approach. In 2017, Bengt C Fellström's team formulated the glucocorticoid drug budesonide into a targeted, sustained-release preparation, allowing the drug to be absorbed at the end of the ileum. This treatment was effective against IgAN.⁴⁵ More importantly, the success of this trial challenged the current treatment strategy for IgAN, by targeting the initial stage of the disease (targeting mucosal B lymphocytes), and provided a new idea for the development of subsequent IgAN therapeutic drugs. The drug was approved by the US FDA in November 2022 and is currently the only drug used clinically to treat IgAN.⁴⁶

The present study is the first to investigate the effect of SH on the cell cycle of spleen T and B lymphocytes. The results clearly showed that SH could exert therapeutic effects on IgAN through blocking splenic lymphocytes at the G0/G1 phase, indicating that SH can act on the early stage of IgAN.

Since J. Erger and N. Hinglais identified IgAN in 1968,⁴⁷ its pathogenesis has been associated with immunity due to the key role of IgA1. After the feasibility of the strategy of depletion of B cells was demonstrated, many research groups attempted to further explore the mechanisms underlying the first stage of IgAN. It is currently believed that B and T cells participate in the production of Gd-IgA1⁴⁸ and play a role in the processes of inflammatory infiltration.⁴⁹ In this study, for the first time, the effect of SH on Jurkat T and Ramos B cells was investigated through in vitro experiments. It turns out that SH can markedly reduce the cell viability of Jurkat T and Ramos B cells but does not affect normal cells such as HUVEC cells. Furthermore, SH can arrest the cell cycle, consistent with the in vivo experiment results. These results strongly suggest that SH possesses a good therapeutic effect and should undergo further development.

Cyclins, identified in 1983 by Tom Evans, have concentrations that vary cyclically during the cell cycle.⁵⁰ Cyclin D1, an important Cyclin, acts during phase G1. Cyclin E1 can facilitate the G1/S phase transition.⁵¹ The Western blot assay proved that SH reduced Cyclin E1 and Cyclin D1 expression in Jurkat T and Ramos B cells. Hence, SH can arrest the cell cycle of T and B cells through regulating Cyclin D1 and Cyclin E1 expression; this may be one aspect of the mechanism of SH on IgAN (Figure 8).

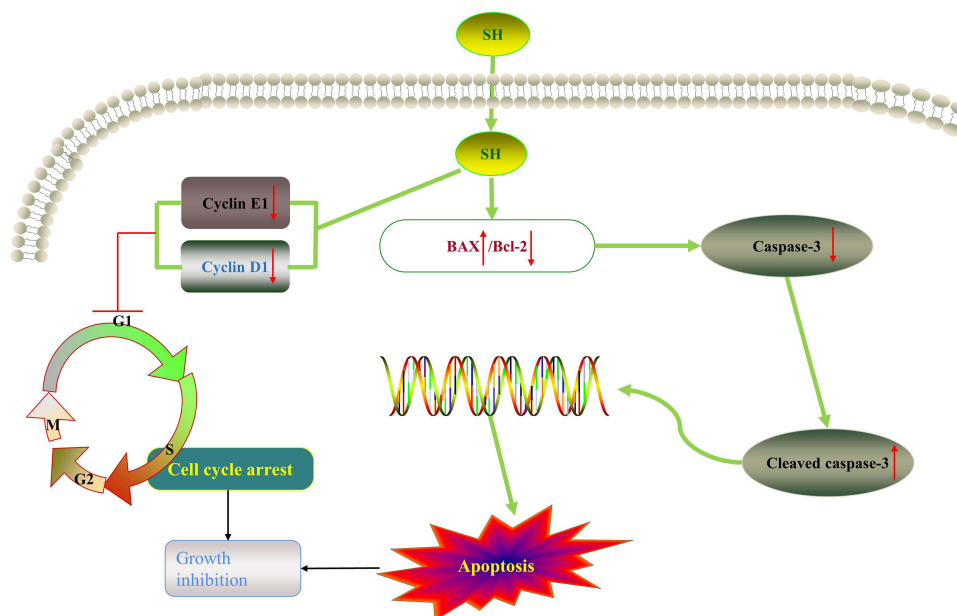


Figure 8 SH possesses therapeutic effects on IgAN through a dual regulation mechanism that inhibits proliferation and induces apoptosis. SH decreases the expression of Cyclin E1 and Cyclin D1, arresting T and B cells at the G0/G1 phase of the cell cycle (in vitro and in the spleen), thus inhibiting growth. Additionally, SH induces apoptosis by up-regulating Bax and down-regulating Bcl-2 expression (which are factors in the mitochondrial apoptosis pathway), and activating Cleaved caspase-3, therefore inhibiting growth.

Apoptosis was initially identified in 1972 by Kerr.⁵² SH can regulate the inflammatory response by inducing apoptosis.⁵³ The study proved that SH can induce Jurkat T and Ramos B cell apoptosis, implying that SH affects IgAN through a dual regulation, by arresting the cell cycle and inducing apoptosis.

Bax and Bcl-2 can regulate mitochondrial function through a synergistic effect with other apoptosis-related factors.⁵⁴ The down-regulation of Bcl-2 protein expression and the up-regulation of Bax protein expression can activate Caspase-3 to Cleaved caspase-3. The Western blot assay confirmed that SH increased Bax and Cleaved caspase-3 protein expression and reduce Bcl-2 and Caspase-3 protein expression. Hence, SH can induce Jurkat T and Ramos B cells apoptosis through regulating Bax, Bcl-2, and Cleaved caspase-3 protein expression; this is another aspect of the mechanism of SH on IgAN (Figure 8).

Conclusion

In conclusion, we confirmed for the first time that SH exerts a favorable therapeutic effect affecting the initial and final stages of IgAN, and preliminarily explained partial mechanisms of SH in the treatment of IgAN. We discovered that SH possesses unique advantages: it can inhibit cell growth through a dual regulation mechanism (inducing apoptosis and arresting the cell cycle) and decrease IgA and C3 deposition as well as pathological changes in the kidney. In addition, Ramos B cells were more sensitive to SH than Jurkat T cells.

Acknowledgments

This work was supported by the Hunan Province Science and Technology Innovation Key Projects (Project No: 2015SK1001, 2020SK1020), the National Natural Science Foundation of China (Project No.: 81803811, 82274178), the Wuxi Young Talent Program of Huaihua City and the Hunan University of Medicine High-Level Talent Introduction Startup Funds.

Disclosure

The authors declare no conflicts of interest in this work.

References

1. Huang C, Li X, Wu J, et al. The landscape and diagnostic potential of T and B cell repertoire in immunoglobulin a nephropathy. *J Autoimmun.* 2019;97:100–107. doi:10.1016/j.jaut.2018.10.018
2. Hotta O, Ieiri N, Nagai M, Tanaka A, Harabuchi Y. Role of palatine tonsil and epipharyngeal lymphoid tissue in the development of glomerular active lesions (glomerular vasculitis) in immunoglobulin a nephropathy. *Int J Mol Sci.* 2022;23:727. doi:10.3390/ijms23020727
3. Park JI, Kim TY, Oh B, et al. Comparative analysis of the tonsillar microbiota in IgA nephropathy and other glomerular diseases. *Sci Rep.* 2020;10(1):16206. doi:10.1038/s41598-020-73035-x
4. Thompson A, Carroll K, L AI, et al. Proteinuria reduction as a surrogate end point in trials of IgA nephropathy. *Clin J Am Soc Nephrol.* 2019;14(3):469–481. doi:10.2215/CJN.08600718
5. Taylor S, Pieri K, Nanni P, Tica J, Barratt J, Didangelos A. Phosphatidylethanolamine binding protein-4 (PEBP4) is increased in IgA nephropathy and is associated with IgA-positive B-cells in affected kidneys. *J Autoimmun.* 2019;105:102309. doi:10.1016/j.jaut.2019.102309
6. Moroni G, Belingeri M, Frontini G, Tamborini F, Messa P. Immunoglobulin A nephropathy. recurrence after renal transplantation. *Front Immunol.* 2019;10:1332. doi:10.3389/fimmu.2019.01332
7. Ohyama Y, Renfrow MB, Novak J, Takahashi K. Aberrantly glycosylated IgA1 in iga nephropathy: what we know and what we don't know. *J Clin Med.* 2021;10(16). doi:10.3390/jcm10163467
8. Xie X, Liu P, Gao L, et al. Renal deposition and clearance of recombinant poly-IgA complexes in a model of IgA nephropathy. *J Pathol.* 2021;254(2):159–172. doi:10.1002/path.5658
9. Seikrit C, Pabst O. The immune landscape of IgA induction in the gut. *Semin Immun.* 2021;43(5):627–637. doi:10.1007/s00281-021-00879-4
10. Bemark M, Angeletti D. Know your enemy or find your friend?-induction of IgA at mucosal surfaces. *Immunol Rev.* 2021;303(1):83–102. doi:10.1111/imr.13014
11. Gesualdo L, Di Leo V, Coppo R. The mucosal immune system and IgA nephropathy. *Semin Immun.* 2021;43(5):657–668. doi:10.1007/s00281-021-00871-y
12. Floege J, Rauen T, Tang SCW. Current treatment of IgA nephropathy. *Semin Immun.* 2021;43(5):717–728. doi:10.1007/s00281-021-00888-3
13. Weiberg D, Basic M, Smoczek M, Bode U, Bornemann M, Buettner M. Participation of the spleen in the IgA immune response in the gut. *PLoS One.* 2018;13(10):e0205247. doi:10.1371/journal.pone.0205247
14. Zheng N, Xie K, Ye H, et al. TLR7 in B cells promotes renal inflammation and Gd-IgA1 synthesis in IgA nephropathy. *JCI Insight.* 2020;5. doi:10.1172/jci.insight.136965
15. Makita Y, Suzuki H, Kano T, et al. TLR9 activation induces aberrant IgA glycosylation via April- and IL-6-mediated pathways in IgA nephropathy. *Kidney Int.* 2020;97(2):340–349. doi:10.1016/j.kint.2019.08.022

16. He JW, Zhou XJ, Lv JC, Zhang H. Perspectives on how mucosal immune responses, infections and gut microbiome shape IgA nephropathy and future therapies. *Theranostics*. 2020;10(25):11462–11478. doi:10.7150/thno.49778
17. Lin Y, Yin P, Zhu Z, et al. Epigenome-wide association study and network analysis for IgA nephropathy from CD19(+) B-cell in Chinese Population. *Epigenetics*. 2021;16(12):1283–1294. doi:10.1080/15592294.2020.1861171
18. Liu Y, Zheng J, Zhao N, Jia J, Yan T. ELL2 Is downregulated and associated with galactose-deficient IgA1 in IgA nephropathy. *Dis Markers*. 2019;2019:2407067. doi:10.1155/2019/2407067
19. Selvaskandan H, Gonzalez-Martin G, Barratt J, Cheung CK. IgA nephropathy: an overview of drug treatments in clinical trials. *Expert Opin Investig Drugs*. 2022;31(12):1321–1338. doi:10.1080/13543784.2022.2160315
20. Zhao Y, Liu H. Mechanism for the therapeutic effect of tripterygium wilfordii hook. f. preparations on IgA nephropathy. *J Cent South Univ*. 2022;47(05):573–582. doi:10.11817/j.issn.1672-7347.2022.210410
21. Zhang W, Yuan Y, Li X, et al. Orange-derived and dexamethasone-encapsulated extracellular vesicles reduced proteinuria and alleviated pathological lesions in IgA nephropathy by targeting intestinal lymphocytes. *Front Immunol*. 2022;13:900963. doi:10.3389/fimmu.2022.900963
22. Wang X, Li T, Si R, Chen J, Qu Z, Jiang Y. Increased frequency of PD-1(hi)CXCR5(-) T cells and B cells in patients with newly diagnosed IgA nephropathy. *Sci Rep*. 2020;10(1):492. doi:10.1038/s41598-019-57324-8
23. Wei SY, Guo S, Feng B, Ning SW, Du XY. Identification of miRNA-mRNA network and immune-related gene signatures in IgA nephropathy by integrated bioinformatics analysis. *BMC Nephrol*. 2021;22(1):392. doi:10.1186/s12882-021-02606-5
24. Du W, Gao CY, You X, et al. Increased proportion of follicular helper T cells is associated with B cell activation and disease severity in IgA nephropathy. *Front Immunol*. 2022;13:901465. doi:10.3389/fimmu.2022.901465
25. Ruszkowski J, Lisowska KA, Pindel M, Heleniak Z, Dębska-Ślizień A, Witkowski JM. T cells in IgA nephropathy: role in pathogenesis, clinical significance and potential therapeutic target. *Clin Exp Nephrol*. 2019;23(3):291–303. doi:10.1007/s10157-018-1665-0
26. Ka SM, Hsieh TT, Lin SH, et al. Decoy receptor 3 inhibits renal mononuclear leukocyte infiltration and apoptosis and prevents progression of IgA nephropathy in mice. *Am J Physiol Renal Physiol*. 2011;301(6):F1218–1230. doi:10.1152/ajprenal.00050.2011
27. Gan L, Li X, Zhu M, Chen C, Luo H, Zhou Q. Acteoside relieves mesangial cell injury by regulating Th22 cell chemotaxis and proliferation in IgA nephropathy. *Ren Fail*. 2018;40(1):364–370. doi:10.1080/0886022x.2018.1450762
28. Liu L, Michowski W, Kolodziejczyk A, Sicinski P. The cell cycle in stem cell proliferation, pluripotency and differentiation. *Nat Cell Biol*. 2019;21(9):1060–1067. doi:10.1038/s41556-019-0384-4
29. Shkarina K, Broz P. Selective induction of programmed cell death using synthetic biology tools. *Semin Cell Dev Biol*. 2023;156:74–92. doi:10.1016/j.semcdb.2023.07.012
30. Zhu L, Dai LM, Shen H, et al. Qing Chang Hua Shi granule ameliorate inflammation in experimental rats and cell model of ulcerative colitis through MEK/ERK signaling pathway. *Biomed Pharmacother*. 2019;116:108967. doi:10.1016/j.biopha.2019.108967
31. Zhang T, Ouyang X, Gou S, et al. Novel synovial targeting peptide-sinomenine conjugates as a potential strategy for the treatment of rheumatoid arthritis. *Int J Pharm*. 2022;617:121628. doi:10.1016/j.ijpharm.2022.121628
32. Liu Y, Sun Y, Zhou Y, et al. Sinomenine hydrochloride inhibits the progression of plasma cell mastitis by regulating IL-6/JAK2/STAT3 pathway. *Int Immunopharmacol*. 2020;81:106025. doi:10.1016/j.intimp.2019.106025
33. Gao WJ, Liu JX, Xie Y, et al. Suppression of macrophage migration by down-regulating Src/FAK/P130Cas activation contributed to the anti-inflammatory activity of sinomenine. *Pharmacol Res*. 2021;167:105513. doi:10.1016/j.phrs.2021.105513
34. Panos GD, Boeckler FM. Statistical analysis in clinical and experimental medical research: simplified guidance for authors and reviewers. *Drug Des Devel Ther*. 2023;17(1959–61):1959–1961. doi:10.2147/DDDT.S427470
35. Festing MF. Design and statistical methods in studies using animal models of development. *ILAR J*. 2006;47(1):5–14. doi:10.1093/ilar.47.1.5
36. He J, Peng F, Chang J, et al. The therapeutic effect of Shenhua tablet against mesangial cell proliferation and renal inflammation in mesangial proliferative glomerulonephritis. *Biomed Pharmacother*. 2023;165:115233. doi:10.1016/j.biopha.2023.115233
37. Lee GH, Hwang KA, Choi KC. Effects of fludioxonil on the cell growth and apoptosis in T and B lymphocytes. *Biomolecules*. 2019;9:9. doi:10.3390/biom9090500
38. Suzuki H, Novak J. IgA glycosylation and immune complex formation in IgAN. *Semin Immunol*. 2021;43(5):669–678. doi:10.1007/s00281-021-00883-8
39. Liu J, Tang X, Xu X, et al. Review on research progress of experimental animal model of IgA nephropathy. *Radi Chin Drug Res Clin Pharm*. 2019;30(02):257–263. doi:10.19378/j.issn.1003-9783.2019.02.021
40. Chang S, Li XK. The role of immune modulation in pathogenesis of IgA nephropathy. *Front Med Lausanne*. 2020;7:92. doi:10.3389/fmed.2020.00092
41. Rizk DV, Maillard N, Julian BA, et al. The emerging role of complement proteins as a target for therapy of IgA nephropathy. *Front Immunol*. 2019;10:504. doi:10.3389/fimmu.2019.00504
42. Yang JYC, Sarwal RD, Fervenza FC, Sarwal MM, Lafayette RA. Noninvasive urinary monitoring of progression in IgA nephropathy. *Int J Mol Sci*. 2019;20:18. doi:10.3390/ijms20184463
43. Tan Q, Xue H, Ni X, Fan L, Du W. Comparative effectiveness and safety for the treatments despite optimized renin-angiotensin system blockade among IgA nephropathy patients at high-risk of disease progression: a network meta-analysis of randomized controlled trials. *Eur J Intern Med*. 2023;114:66–73. doi:10.1016/j.ejim.2023.04.022
44. Vaz de Castro PAS, Bitencourt L, Pereira BWS, et al. Efficacy and safety of angiotensin-converting enzyme inhibitors or angiotensin receptor blockers for IgA nephropathy in children. *Pediatr Nephrol*. 2022;37(3):499–508. doi:10.1007/s00467-021-05316-0
45. Fellström BC, Barratt J, Cook H, et al. Targeted-release budesonide versus placebo in patients with IgA nephropathy (NEFIGAN): a double-blind, randomised, placebo-controlled phase 2b trial. *Lancet*. 2017;389(10084):2117–2127. doi:10.1016/S0140-6736(17)30550-0
46. Barratt J, Lafayette R, Kristensen J, et al. Results from part A of the multi-center, double-blind, randomized, placebo-controlled NefIgArd trial, which evaluated targeted-release formulation of budesonide for the treatment of primary immunoglobulin A nephropathy. *Kidney Int*. 2023;103(2):391–402. doi:10.1016/j.kint.2022.09.017
47. Haraldsson B. Phase 3 trial results bring hope for patients with IgA nephropathy. *Lancet*. 2023;402:827–829. doi:10.1016/S0140-6736(23)01633-1
48. Liang Y, Zeng Q, Wang XH, Yan L, Yu RH. Mechanism of Yiqi Yangying Heluo formula in the treatment of IgA nephropathy by affecting Gd-IgA1 based on BAFF molecular level and T lymphocyte immunity. *Biomed Res Int*. 2023;2023:5124034. doi:10.1155/2023/5124034

49. Tang R, Meng T, Lin W, et al. A Partial Picture of the single-cell transcriptomics of human IgA Qropathy. *Front Immunol.* 2021;12:645988. doi:10.3389/fimmu.2021.645988
50. Gorski JW, Ueland FR, Kolesar JM. CCNE1 amplification as a predictive biomarker of chemotherapy resistance in epithelial ovarian cancer. *Diagnostics.* 2020;10:5. doi:10.3390/diagnostics10050279
51. Fagundes R, Teixeira LK. Cyclin E/CDK2: DNA replication, replication stress and genomic instability. *Front Cell Dev Biol.* 2021;9:774845. doi:10.3389/fcell.2021.774845
52. McArthur K, Kile BT. Apoptotic mitochondria prime anti-tumour immunity. *Cell Death Discov.* 2020;6(1):98. doi:10.1038/s41420-020-00335-6
53. Zhang MW, Wang XH, Shi J, Yu JG. Sinomenine in cardio-cerebrovascular diseases: potential therapeutic effects and pharmacological evidences. *Front Cardiovasc Med.* 2021;8:749113. doi:10.3389/fcvm.2021.749113
54. Czabotar PE, Garcia-Saez AJ. Mechanisms of BCL-2 family proteins in mitochondrial apoptosis. *Nat Rev Mol Cell Biol.* 2023;24:732–748. doi:10.1038/s41580-023-00629-4

Drug Design, Development and Therapy

Dovepress

Publish your work in this journal

Drug Design, Development and Therapy is an international, peer-reviewed open-access journal that spans the spectrum of drug design and development through to clinical applications. Clinical outcomes, patient safety, and programs for the development and effective, safe, and sustained use of medicines are a feature of the journal, which has also been accepted for indexing on PubMed Central. The manuscript management system is completely online and includes a very quick and fair peer-review system, which is all easy to use. Visit <http://www.dovepress.com/testimonials.php> to read real quotes from published authors.

Submit your manuscript here: <https://www.dovepress.com/drug-design-development-and-therapy-journal>